Monatsh Chem (2011) 142:827–836
DOI 10.1007/s00706-011-0515-5

ORIGINAL PAPER

Synthesis of Diels–Alder adducts of *N*-arylmaleimides by a multicomponent reaction between maleic anhydride, dienes, and anilines

J. Alberto Guevara-Salazar · Delia Quintana-Zavala · Hugo A. Jiménez-Vázquez · José Trujillo-Ferrara

Received: 26 October 2010 / Accepted: 26 April 2011 / Published online: 31 May 2011

Abstract We have carried out the synthesis and characterization of some hexahydroisoindolyl benzoic acids and their corresponding ethyl esters by a multicomponent reaction (MCR) between aminobenzoic acids or aminobenzoates, maleic anhydride, and isoprene in the absence of catalysts. According to additional experiments, the MCR takes place by sequential formation of *N*-arylmaleamic acids from the aminobenzoic acids or aminobenzoates and maleic anhydride, Diels–Alder adducts of the acids and isoprene, and finally the imides. The ^{1}H NMR data (coupling constants) of the adducts suggested that the preferred conformation of the corresponding cyclohexene rings is a *syn*-boat, a fact supported by a density functional theory (DFT) conformational analysis and DFT calculations of the spin–spin coupling constants of the corresponding conformers. Our MCR synthetic methodology was tested successfully in the synthesis of other adducts, for which cyclopentadiene and other anilines were employed.

Keywords Cycloadditions · Conformation · Cyclizations · Hexahydroisoindolediones · Computational chemistry

Electronic supplementary material The online version of this article (doi:10.1007/s00706-011-0515-5) contains supplementary material, which is available to authorized users.

J. A. Guevara-Salazar · H. A. Jiménez-Vázquez
Departamento de Química Orgánica, Escuela Nacional de Ciencias Biológicas, Instituto Politécnico Nacional, Prol. Carpio y Plan de Ayala s/n, 11340 Mexico, DF, Mexico

D. Quintana-Zavala
Laboratorio de Química Orgánica, Centro de Investigación en Ciencia Aplicada y Tecnología Avanzada, Instituto Politécnico Nacional, Calzada Legaria No. 694, 11500 Mexico, DF, Mexico

J. A. Guevara-Salazar · J. Trujillo-Ferrara (✉)
Departamento de Bioquímica, Escuela Superior de Medicina, Instituto Politécnico Nacional, Salvador Díaz Mirón y Plan de San Luis s/n, 11340 Mexico, DF, Mexico
e-mail: jtrujillo@ipn.mx

Introduction

Reactions that involve three or more components in a single synthetic step are useful in the synthesis of relatively simple or structurally complex organic molecules [1]. These reactions are known, in general, as multicomponent reactions (MCR); they also include one-pot reactions, in which additional components are added to the reaction mixture at subsequent stages. One of the advantages of these MCR is that they eliminate the need for work-up and purification at each of the reaction steps, making the overall process faster, and reducing the amount of solvent used. In this sense, Diels–Alder reactions are no exception, as several examples of MCR involving thermal [2–4] and catalyzed [5, 6] cycloaddition reactions have been reported.

The Diels–Alder cycloaddition reactions of *N*-substituted maleimides as dienophiles have been carried out with a number of different dienes and under different methodologies [7], including the use of chiral [8, 9] and achiral catalysts [10], Lewis acid catalysts [11], under heating [11], or even at room temperature [12, 13]. Other variations employed for these cycloadditions involve the use of aqueous buffer solutions [14] or microwaves [15], which have led to good results in terms of the decrease in the overall reaction time.

Herein we introduce an MCR between maleic anhydride, isoprene, and aminobenzoic acids or ethyl aminobenzoates, in which the final product is that expected from the [4 + 2] Diels–Alder cycloaddition of the corresponding *N*-arylmaleimides and isoprene; in this three-

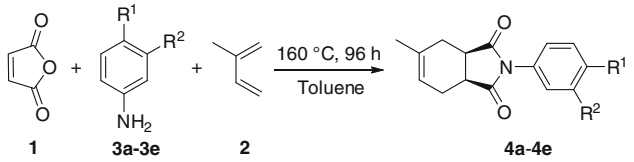

a: R^1 = COOH, R^2 = H
b: R^1 = COOEt, R^2 = H
c: R^1 = H, R^2 = COOH
d: R^1 = H, R^2 = COOEt
e: R^1 = H, R^2 = H

Scheme 1

component MCR no catalyst was used. We also carried out, independently, the preparation of the same adducts in a conventional synthesis in order to make a direct comparison between both methods, and propose the most likely sequence of events taking place within the MCR. In addition, from the $^3J_{HH}$ coupling constants of the adducts and from data derived from density functional theory (DFT) calculations we have determined the preferred conformation of the fused bicyclic system.

Results and discussion

Carboxylic acids **4a** and **4c** and the corresponding ethyl esters **4b** and **4d** were synthesized by an MCR between maleic anhydride (**1**), isoprene (**2**), and the corresponding *para*- or *meta*-aminobenzoic acids or ethyl aminobenzoates (**3a**–**3d**) in toluene under thermal conditions (Scheme 1). In all cases a single product was detected by TLC and purified by recrystallization from CH_2Cl_2/*n*-hexane. The characterization of these products was carried out by spectroscopy, particularly by ^{1}H and ^{13}C one- and two-dimensional NMR. As shown in Table 1, the yields obtained in our MCR range from good to excellent.

The ^{1}H and ^{13}C chemical shifts of the products and the coupling patterns of the ^{1}H signals are in agreement with those expected for compounds **4**. The coupling constants ($^3J_{HH}$) of the aliphatic protons of the cyclohexene ring of adduct **4b** were assigned directly from the corresponding spectrum, according to the numbering shown in Scheme 2.

Even though it is usually assumed that the most stable conformers of a cyclohexene ring would be half-chairs [16, 17], it is known that in *cis*-fused [4.3.0]bicyclic systems, such as the hexahydroisoindole nucleus of our adducts, the most stable conformation is a boat [17]. However, from NMR data it has been proposed that out of the two possible boat forms (*syn* and *anti*, see below), the predominance of one over the other depends on the particular structure of the system under study [18–23], a fact supported by crystallographic data [24–26].

Table 1 Yields of adducts **4** obtained through the MCR

Product	Yield (%)
4a	90.7
4b	71.9
4c	76.9
4d	96.2

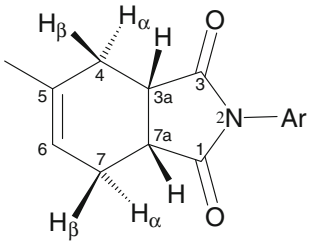

Scheme 2

In the particular case of **4b**, protons H3a and H7a show three coupling constants each; the first corresponds to the interaction between them: $J_{H3aH7a} = 9.38$ Hz. In addition, the other two coupling constants involving H3a and the diasterotopic H4α,4β protons have values of 2.50 and 7.25 Hz. The coupling constants between H7a and the H7α,7β protons are very similar to the former set, 2.50 and 6.60 Hz. The geminal ($^2J_{HH}$) coupling constants between the H4α,4β and the H7α,7β protons are both around 15.5 Hz. The fact that the coupling constants between the bridge protons and the adjacent α and β methylene protons are so different suggests the predominance of a single conformer. Furthermore, it does not agree with the idea of a half-chair as the major conformer, because there is no apparent reason why one of the two possible half-chair conformations would be preferred over the other. It is likely that conformational averaging between the two half-chair forms would lead to less dissimilar values of these coupling constants.

To further investigate the preferred conformation of adducts **4**, we carried out theoretical calculations with Gaussian 09 [27] on some of the possible conformers of adduct **4b**, in the context of DFT, using the 6-31+G(d,p) basis set in combination with Truhlar's meta-GGA M06-2X hybrid functional [28, 29]. As the NMR data was obtained in $CDCl_3$, we also introduced the effect of solvation (chloroform, $\varepsilon = 4.7113$) through Tomasi's polarizable continuum model (PCM) model [30], as implemented in the default self-consistent reaction field (SCRF) methodology of Gaussian 09 [31]; optimizations and vibrational frequency analyses were carried out under the effect of solvation at this level of theory. The optimized geometries of the conformers investigated, two boats (*b-syn* and *b-anti*) and two half-chairs (*hc-1* and *hc-2*), are

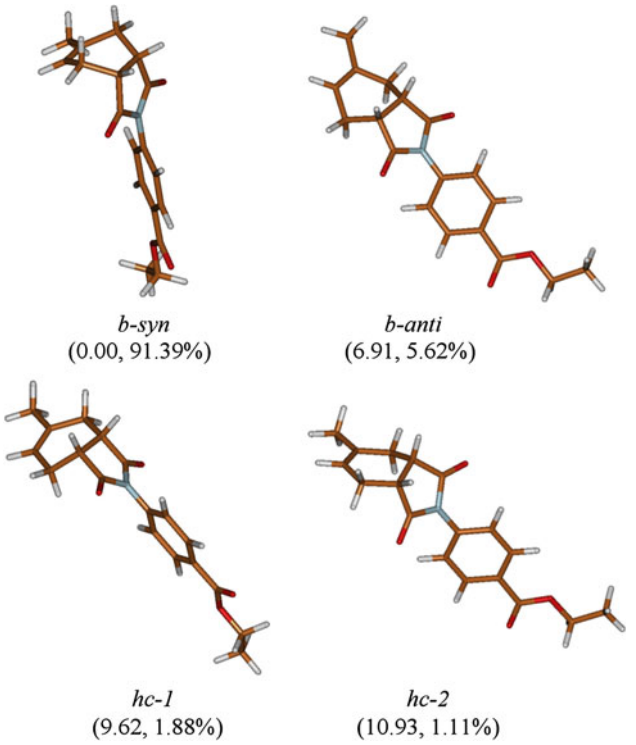

Fig. 1 M06-2X/6-31+G(d,p)/PCM optimized geometries, calculated relative free energies (ΔG at 25 °C kJ/mol), and proportions of the conformers assuming a Boltzmann distribution of the boat (*b*) and half-chair (*hc*) geometries of adduct **4b**

shown in Fig. 1 in order of relative free energies (calculated at 25 °C). We did not explore the conformations of the phenyl ring or the carboethoxy group. Supported by the NMR data of adducts **4a**–**4d**, we assumed that the conformation of the bicyclic moiety was essentially independent of the geometry of these fragments. Interestingly enough, from the calculations the most stable conformers turned out to be the boat forms. Most likely this is the result of the strain introduced into the cyclohexene ring by the *cis*-fused five-membered ring in the half-chair conformations. The fact that the most stable boat conformer (*b-syn*) is that in which both carbonyl carbons of the heterocyclic ring have the axial orientation, can be explained in terms of a lower torsional strain arising from the interaction of these carbons with the C4/C7α methylene protons, with respect to conformer *b-anti*.

For all four conformers we determined the relevant H–C–C–H dihedral angles, and from them we estimated the corresponding empirical vicinal coupling constants according to the Haasnoot–de Leeuw–Altona equation [32], as implemented in the ALTONA computer program [33]. In addition, we also calculated the theoretical spin–spin coupling constants from DFT data, employing the two-step methodology described by Deng et al. [34] as implemented in Gaussian 09, at the B3LYP/6-311+G(d,p) level of theory under solvation effects (PCM) on the M06-2X/6-31+G(d,p)/PCM geometries previously obtained. Furthermore, from both sets of calculated coupling constants (empirical and DFT) and the relative energies of the conformers, we also estimated two sets of calculated average coupling constants (empirical and theoretical) assuming a Boltzmann distribution of conformers, according to methodology described elsewhere [35]. The results are summarized in Fig. 1 and in Table 2.

Notice that the theoretical calculation also allows for the estimation of the $^2J_{HH}$ coupling constants for H4α–H4β and H7α–H7β. In Table 3 we present the average values of these coupling constants compared with the experimental ones.

It can be seen that the ^3J (and ^2J) experimental values are more similar to those of the most stable conformer *b-syn*. However, the agreement is even better if we consider the averaged coupling constant values. In addition, it is readily apparent that the values derived from the DFT calculations of spin–spin coupling are in even better agreement than the empirical ones. Thus, we can conclude that indeed the most stable conformer of the cyclohexene fragment in adducts **4**, in the gas phase as well as in solution, is the *syn*-boat.

Table 2 Dihedral angles (θ°), empirical (emp), and theoretical (theor) coupling constants ($^3J_{HH}$, Hz) derived from the M06-2X/6-31+G(d,p)/PCM optimized geometries of the boat (*b*) and half-chair (*hc*) conformers of adduct **4b** (see text)

Conformer	H3a–H7a θ	H3a–H4α θ	H3a–H4β θ	H7a–H7α θ	H7a–H7β θ
b-syn	1.8	65.7	−50.8	−68.2	47.9
b-anti	2.2	159.1	42.7	−161.2	−44.8
hc-1	37.7	95.6	−19.1	−152.8	−37.6
hc-2	−37.8	152.5	37.2	−94.5	20.3
emp	^3J	^3J	^3J	^3J	^3J
b-syn	11.1	2.2	4.3	2.0	4.8
b-anti	11.1	11.1	6.0	11.3	5.6
hc-1	6.9	1.2	9.3	10.2	6.8
hc-2	6.9	10.2	7.0	1.1	9.1
theor	^3J	^3J	^3J	^3J	^3J
b-syn	10.2	2.1	7.7	1.7	8.2
b-anti	11.0	12.5	8.2	12.6	7.8
hc-1	8.7	0.94	11.8	11.0	8.6
hc-2	8.6	11.1	8.7	0.9	11.5
exp	9.40	2.50	7.25	2.50	6.60
avg (emp)	11.0	2.8	4.6	2.7	5.0
avg (theor)	10.2	2.7	7.9	2.5	8.2

The experimental (*exp*) ^3J values are shown for comparison with the values estimated from the Boltzmann distribution of conformers (*avg*)

Table 3 Theoretical coupling constants ($^2J_{HH}$, Hz) derived from the M06-2X/6-31+G(d,p)/PCM optimized geometries of the boat (*b*) and half-chair (*hc*) conformers of adduct **4b** (see text)

Conformer	H4α–H4β ^2J	H7α–H7β ^2J
b-syn	−15.61	−15.91
b-anti	−15.88	−15.73
hc-1	−21.32	−19.18
hc-2	−19.10	−21.64
avg	−15.77	−16.02
exp	15.5	15.5

The experimental (*exp*) ^2J values are shown for comparison with the values estimated from the Boltzmann distribution of conformers (*avg*)

Table 4 Yields obtained in the synthesis of maleamic acids **5** and adducts **4**, according to the reactions displayed in Scheme 3

Product	Yield (%)	Overall yield (%)
5a	90.3	–
5b	89.0	–
5c	95.8	–
5d	77.7	–
4a	76.8	69.4
4b	82.7	73.6
4c	90.2	86.4
4d	64.2	49.9

The overall yields of the two steps are also shown

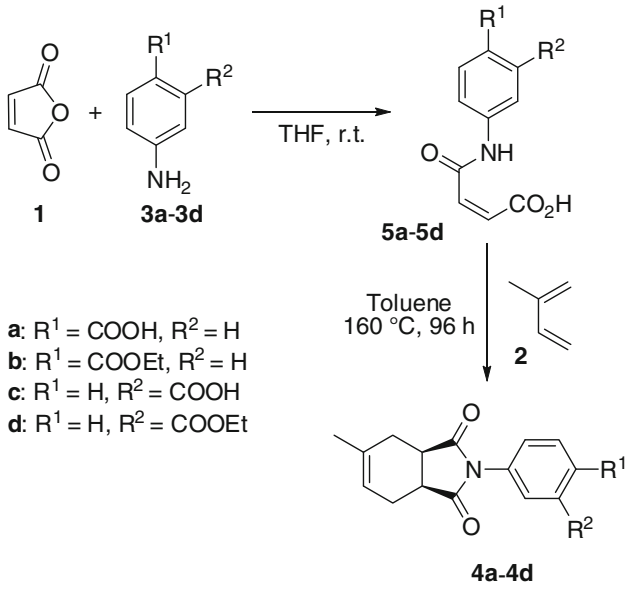

Scheme 3

In order to investigate the sequence of events taking place in our MCR, we carried out the synthesis of adducts **4a**–**4d** through a two-step sequence (Scheme 3). The first reaction involved the synthesis of *N*-arylmaleamic acids, which have been obtained by a number of methodologies [36–43]. In our particular case we followed that described by Trujillo-Ferrara et al. [42, 43], which employs anilines and maleic anhydride. We carried out the reactions in THF as solvent and at room temperature, conditions under which acids **5a**–**5d** were obtained in very good yields (Table 3). THF was employed because the reactants are not soluble in toluene at this temperature. The fact that the reactions took place readily suggests that the formation of the maleamic acids is indeed the first step of the MCR.

In the second reaction, acids **5a**–**5d** react with isoprene under thermal conditions, leading to adducts **4a**–**4d** with global yields for the two steps (Table 4) that are similar to those obtained through the MCR. It is readily apparent that, at least for the synthesis of adducts **4a** and **4d**, we obtained a much better yield in the MCR than in the two-step process (Table 1).

It is interesting to note that under the conditions employed in this second step the cycloaddition takes place simultaneously with the formation of the imide; thus, it is not known which of the two reactions takes place first. In order to investigate this, the second reaction was performed again, under a different set of conditions. In this case, we carried out the reaction of acid **3a** with isoprene in ethyl acetate as solvent at 60 °C for 120 h (toluene was not employed because the maleamic acids **5** are not soluble at this temperature). This time two types of compounds were identified and isolated from the reaction mixture, one being the known adduct **4a**, and the other a mixture of regioisomeric adducts resulting from the cycloaddition of isoprene with **3a** (**6a/7a**, Scheme 4). The presence of the latter was evidenced by two new signals appearing approximately at 10.0 ppm in the ^{1}H NMR spectrum, indicative of the amide groups of the new adducts, which do not exist in adducts **4**. In addition, the ^{1}H and ^{13}C

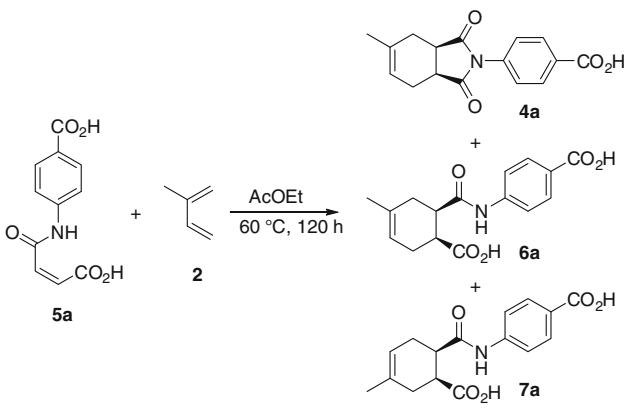

Scheme 4

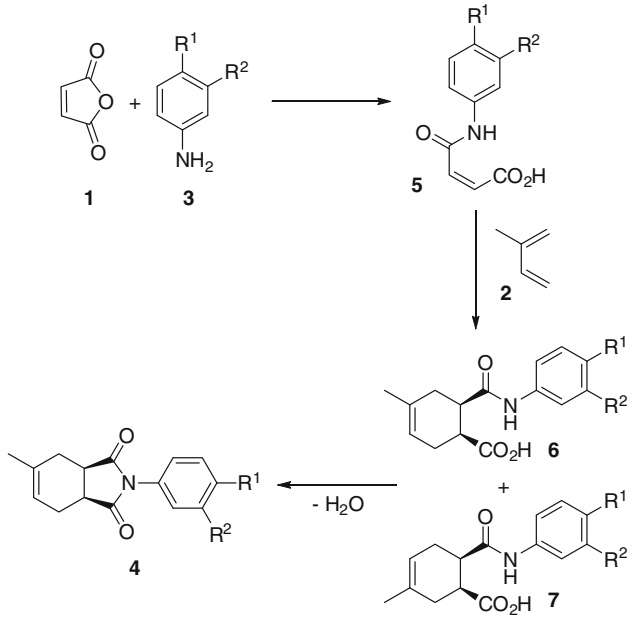

Scheme 5

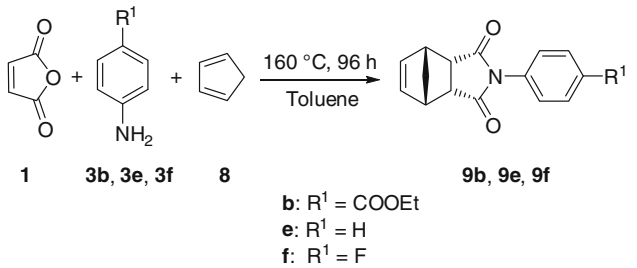

Scheme 6

spectra of the mixture showed two sets of very similar signals for the cyclohexene ring, particularly for the vinylic proton, in a 55:45 proportion.

From the above information, we can propose that the most likely sequence of events taking place in our MCR is that shown in Scheme 5. Maleic anhydride (**1**) reacts rapidly under the reaction conditions with the anilines **3** to yield the corresponding maleamic acids. These intermediates undergo a Diels–Alder cycloaddition with isoprene (**2**) leading to a mixture of adducts **6** and **7**, which cyclize to form imides **4**.

In order to test the generality of our MCR methodology, we carried out additional experiments. The reaction of aniline **3e** with isoprene and maleic anhydride under the conditions described above led to the formation of **4e** in 73% yield (Scheme 1). In a second set of experiments, we performed the reactions between maleic anhydride, cyclopentadiene (**8**), and anilines **3b**, **3e**, or **3f**, which furnished

Table 5 Yields obtained in the MCR synthesis of adducts **4e**, **9b**, **9e**, and **9f** according to the reactions displayed in Schemes 1 and 6

Product	Yield (%)
4e	73.2
9b	75.2
9e	83.5
9f	89.9

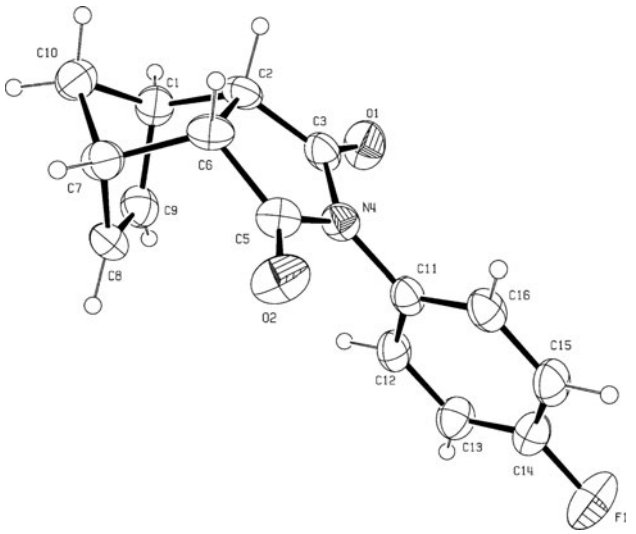

Fig. 2 Oak Ridge thermal ellipsoid plot (ORTEP) of the structure obtained by single-crystal X-ray diffraction of adduct **9f**. Thermal ellipsoids drawn at 30% probability

the corresponding *endo* adducts **9**, also in good yields (Scheme 6); these results are summarized in Table 5.

The *endo* stereochemistry of these adducts was further supported by a single-crystal X-ray diffraction analysis carried out on a crystal of **9f**. The corresponding structure is shown in Fig. 2.

Conclusions

The synthesis of adducts **4a**–**4d** took place in a straightforward manner and in good to excellent yields through a three-component MCR. The spectroscopic data are in full agreement with the proposed structures. The NMR data suggested that the preferred conformation in the cyclohexene fragment of these adducts is a boat, a fact that was supported by the comparison with coupling constants derived from empirical methods and theoretical calculations. It is readily apparent that the calculation of the theoretical spin–spin coupling constants and the inclusion of solvation led to a better agreement between experimental and calculated values. The synthesis of **4a**–**4d** was

also carried out in a two-step process; in this case, although the yields of **4b** and **4c** were comparable to those obtained in the MCR, the yields of **4a** and **4d** were much lower. Our MCR methodology also allowed for the synthesis of adducts **4e**, **9b**, **9e**, and **9f** in good yields, for which different anilines and dienes were used. For the particular case of adducts **9**, they were obtained with *endo* stereochemistry, as evidenced by X-ray diffraction. The MCR has additional advantages in terms of the overall shorter reaction times, lower cost, and lower environmental impact, as a result of the reduced amounts of solvents and reactants used.

Experimental

All reagents and solvents, except THF and AcOEt, were purchased and used without additional purification. THF was distilled from a deep-blue solution of the solvent containing sodium and benzophenone under nitrogen atmosphere. Ethyl acetate was purified by fractional distillation. Cyclopentadiene was obtained by distillation from bicyclopentadiene and used a short time after. Analytical thin-layer chromatography (TLC) was carried out on Merck-DC-F254 aluminum plates, using short-wave UV light for visualization. The melting points were determined in a Mel-Temp II apparatus. The IR spectra were determined in KBr discs, or in solution ($CHCl_3$) for liquid samples, in a Spectrum One FT-IR spectrophotometer. The IR absorption frequencies are reported in cm^{-1}. The UV–Vis spectra were determined in a UV–Vis Beackman Coulter DU 650 spectrophotometer, using CH_3OH or CH_2Cl_2 as solvents. The ^1H and ^{13}C NMR spectra were obtained in a Varian VNMRS-500 spectrometer, at 500 MHz (125.787 MHz for ^{13}C), or in a Varian Mercury spectrometer operating at 300 MHz (75 MHz for ^{13}C). The samples were dissolved in $CDCl_3$ or DMSO-d_6, using TMS as internal reference. HRMS data were obtained in a JEOL GCmateTM II spectrometer in electron impact (EI, 70 eV) mode.

*General method for the preparation of Diels–Alder adducts **4a–4e**, **9b**, **9e**, and **9f** by MCR*

The corresponding aniline **3a–3f** (250 mg) together with 1 equivalent of maleic anhydride (**1**) and 2 equivalents of isoprene (**2**) and 9.0 cm^3 of toluene were deposited in a 20-cm^3 ACE pressure tube. The tube was closed, introduced into a sand bath at 160 °C, and kept under constant stirring for 96 h. After this time the product was precipitated with cold *n*-hexane, filtered, and washed twice with 20 cm^3 of *n*-hexane at room temperature (r.t.). The product was purified and characterized by spectroscopy. ^1H and ^{13}C spectra of these adducts as well as detailed NMR data of known compounds **4e**, **9e**, and **9f** are presented in the Supplementary Material.

4-[(3aR,7aS*)-1,3,3a,4,7,7a-Hexahydro-5-methyl-1,3-dioxo-2H-isoindol-2-yl]benzoic acid* (**4a**, $C_{16}H_{15}NO_4$)
From the general method, with 250 mg of **3a** (1.823 mmol), 178.8 mg of **1** (1.823 mmol), and 0.37 cm^3 of **2** (3.646 mmol); the product was recrystallized from a cold mixture of CH_2Cl_2/*n*-hexane, leading to a white powder in 90.7% yield (471.7 mg, 1.653 mmol). M.p.: 178–180 °C; $R_f = 0.15$ (*n*-hexane/AcOEt 6:4); UV–Vis (CH_2Cl_2): λ_{max} (ε) = 245.3 ± 0.8 (13,765.8) nm (mol^{-1} dm^3 cm^{-1}); IR (KBr):$\bar{\nu}$ = 3,437, 2,935, 1,712, 1,456 cm^{-1}; ^1H NMR (500 MHz, $CDCl_3$): δ = 8.20 (2H, d, ^3J = 8.50 Hz), 7.42 (2H, d, ^3J = 8.50 Hz), 5.63 (1H, br), 3.30 (1H, ddd, ^3J = 9.51 Hz, ^3J = 6.68 Hz, ^3J = 2.50 Hz), 3.25 (1H, ddd, ^3J = 9.51 Hz, ^3J = 7.50 Hz, ^3J = 2.50 Hz), 2.66 (^1H, ddd, ^2J = 15.50 Hz, ^3J = 6.68 Hz, ^3J = 2.50 Hz), 2.60 (1H, dd, ^2J = 15.50 Hz, ^3J = 2.50 Hz), 2.33 (1H, m), 2.28 (1H, m), 1.78 (3H, s) ppm; ^{13}C NMR (125 MHz, $CDCl_3$): δ = 179.2, 179.0, 171.2, 137.0, 136.8, 131.2, 129.3, 126.5, 120.4, 40.0, 39.6, 29.1, 24.7, 23.7 ppm; HRMS (EI): *m/z* calculated for $C_{16}H_{15}NO_4$ [M^+] 285.1001, found 285.0978.

Ethyl 4-[(3aR,7aS*)-1,3,3a,4,7,7a-hexahydro-5-methyl-1,3-dioxo-2H-isoindol-2-yl]benzoate* (**4b**, $C_{18}H_{19}NO_4$)
From the general method, with 250 mg of **3b** (1.513 mmol), 148.4 mg of **1** (1.513 mmol), and 0.30 cm^3 of **2** (3.027 mmol); the product was recrystallized from a cold mixture of CH_2Cl_2/*n*-hexane, leading to a white powder in 71.9% yield (341.0 mg, 1.088 mmol). M.p.: 139–140 °C; $R_f = 0.55$ (*n*-hexane/AcOEt 6:4); UV–Vis (CH_2Cl_2): λ_{max} (ε) = 243.4 ± 0.1 (14,641.8) nm (mol^{-1} dm^3 cm^{-1}); IR (KBr): $\bar{\nu}$ = 3,450, 2,939, 1,709, 1,456 cm^{-1}; ^1H NMR (500 MHz, $CDCl_3$): δ = 8.12 (2H, d, ^3J = 8.75 Hz), 7.36 (2H, d, ^3J = 8.75 Hz), 5.61 (1H, br), 4.38 (2H, q), 3.28 (1H, ddd, ^3J = 9.38 Hz, ^3J = 6.62 Hz, ^3J = 2.50 Hz), 3.21 (1H, ddd, ^3J = 9.38 Hz, ^3J = 7.25 Hz, ^3J = 2.50 Hz), 2.64 (1H, ddd, ^2J = 15.50 Hz, ^3J = 6.62 Hz, ^3J = 2.50 Hz), 2.58 (1H, dd, ^2J = 15.50 Hz, ^3J = 2.50 Hz), 2.35 (1H, m), 2.28 (1H, m), 1.77 (3H, s), 1.39 (3H, t) ppm; ^{13}C NMR (125 MHz, $CDCl_3$): δ = 180.0, 178.2, 166.0, 136.8, 136.2, 130.6, 130.5, 126.3, 120.4, 61.4, 40.0, 39.5, 29.1, 24.7, 23.7, 14.5 ppm; HRMS (EI): *m/z* calculated for $C_{18}H_{19}NO_4$ [M^+] 313.1314, found 313.1324.

3-[(3aR,7aS*)-1,3,3a,4,7,7a-Hexahydro-5-methyl-1,3-dioxo-2H-isoindol-2-yl]benzoic acid* (**4c**, $C_{16}H_{15}NO_4$)
From the general method, with 250 mg of **3c** (1.823 mmol), 178.8 mg of **1** (1.823 mmol), and 0.37 cm^3 of **2**

(3.646 mmol); the product was recrystallized from a cold mixture of CH_2Cl_2/*n*-hexane, leading to a white powder in 76.9% yield (399.9 mg, 1.402 mmol). M.p.: 197–199 °C; $R_f = 0.15$ (*n*-hexane/AcOEt 6:4); UV–Vis (CH_2Cl_2): λ_{max} (ε) = 234.4 ± 1.5 (10,199.5) nm (mol^{-1} dm^3 cm^{-1}); IR (KBr): $\bar{\nu}$ = 3,451, 2,929, 1,706, 1,454 cm^{-1}; ^{1}H NMR (500 MHz, $CDCl_3$): δ = 8.13 (1H, d, ^3J = 7.50 Hz), 8.01 (1H, s), 7.58 (1H, t), 7.51 (1H, d, ^3J = 8.55 Hz), 5.65 (1H, br), 3.32 (1H, ddd, ^3J = 8.20 Hz, ^3J = 7.25 Hz, ^3J = 2.62 Hz), 3.26 (1H, ddd, ^3J = 8.10 Hz, ^3J = 7.94 Hz, ^3J = 2.62 Hz), 2.67 (1H, ddd, ^2J = 15.38 Hz, ^3J = 7.25 Hz, ^3J = 2.25 Hz), 2.61 (1H, dd, ^2J = 15.38 Hz, ^3J = 7.94 Hz), 2.34 (1H, dd, ^2J = 15.50 Hz, ^3J = 7.50 Hz), 2.30 (1H, m), 1.80 (3H, s) ppm; ^{13}C NMR (125 MHz, $CDCl_3$): δ = 179.5, 179.3, 171.0, 136.8, 132.7, 131.9, 130.8, 130.4, 129.6, 128.4, 120.4, 40.0, 39.6, 29.1, 24.7, 23.7 ppm; HRMS (EI): *m*/*z* calculated for $C_{16}H_{15}NO_4$ [M^+] 235.1001, found 285.1001.

Ethyl 3-[(3aR,7aS*)-1,3,3a,4,7,7a-hexahydro-5-methyl-1,3-dioxo-2H-isoindol-2-yl]benzoate* (**4d**, $C_{18}H_{19}NO_4$)

From the general method, with 250 mg of **3d** (1.513 mmol), 148.4 mg of **1** (1.513 mmol), and 0.30 cm^3 of **2** (3.027 mmol); the product was dissolved with CH_2Cl_2 and filtered through a layer of silica gel. The solvent was removed under vacuum in a rotary evaporator, leaving a translucent yellow liquid in 96.2% yield (456.2 mg, 1.456 mmol). $R_f = 0.54$ (*n*-hexane/AcOEt 6:4); UV–Vis (CH_2Cl_2): λ_{max} (ε) = 231.3 ± 1.4 (10,965.1) nm (mol^{-1} dm^3 cm^{-1}); IR ($CHCl_3$): $\bar{\nu}$ = 3,451, 2,938, 1,712, 1,450 cm^{-1}; ^{1}H NMR (500 MHz, $CDCl_3$): δ = 7.98 (1H, d, ^3J = 9.15 Hz), 7.86 (1H, s), 7.45 (1H, t), 7.36 (1H, d, ^3J = 9.15 Hz), 5.54 (1H, br), 4.29 (2H, q), 3.18 (1H, ddd, ^3J = 9.38 Hz, ^3J = 6.80 Hz, ^3J = 2.50 Hz), 3.12 (1H, ddd, ^3J = 9.38 Hz, ^3J = 6.80 Hz, ^3J = 2.50 Hz), 2.54 (1H, ddd, ^2J = 15.62 Hz, ^3J = 6.80 Hz, ^3J = 2.50 Hz), 2.48 (1H, dd, ^2J = 15.50 Hz, ^3J = 2.50 Hz), 2.20 (1H, dd, ^2J = 15.50 Hz, ^3J = 7.13 Hz), 2.16 (1H, m), 1.69 (3H, s), 1.30 (3H, t) ppm; ^{13}C NMR (125 MHz, $CDCl_3$): δ = 179.3, 179.2, 163.7, 136.7, 132.6, 131.8, 131.0, 129.6, 129.3, 127.8, 120.4, 61.5, 39.9, 39.5, 29.0, 24.6, 23.6, 14.5 ppm; HRMS (EI): *m*/*z* calculated for $C_{18}H_{19}NO_4$ [M^+] 313.1314, found 313.1324.

(3aR,7aS*)-3a,4,7,7a-Tetrahydro-5-methyl-2-phenyl-1H-isoindole-1,3(2H)-dione* (**4e**)

From the general method, with 0.25 cm^3 of **3e** (2.68 mmol), 263 mg of **1** (2.68 mmol), and 0.55 cm^3 of **2** (5.36 mmol); the product was recrystallized from a cold mixture of CH_2Cl_2/*n*-hexane, leading to a yellow powder in 73.2% yield (474 mg, 1.96 mmol). M.p.: 83–85 °C (Ref. [44] 85–87 °C).

Ethyl 4-[(3aR,4S*,7R*,7aS*)-1,3,3a,4,7,7a-hexahydro-1,3-dioxo-4,7-methano-2H-isoindol-2-yl]benzoate* (**9b**, $C_{18}H_{17}NO_4$)

From the general method, with 250 mg of **3b** (1.51 mmol), 148 mg of maleic anhydride (1.51 mmol), and 0.25 cm^3 of cyclopentadiene (**8**, 3.02 mmol); the product was recrystallized from a cold mixture of CH_2Cl_2/*n*-hexane, leading to a beige powder in 75.2% yield (354 mg, 1.14 mmol). M.p.: 130–132 °C; $R_f = 0.46$ (*n*-hexane/AcOEt 6:4); IR (KBr): $\bar{\nu}$ = 2,941, 1,731, 1,609, 1,510, 1,478, 1,278, 857, 768 cm^{-1}; ^{1}H NMR (300 MHz, $CDCl_3$): δ = 8.08 (2H, d, ^3J = 8.40 Hz), 7.23 (2H, d, ^3J = 8.40 Hz), 6.25 (2H, br), 4.36 (2H, q, ^3J = 7.10 Hz), 3.49 (2H, m), 3.43 (2H, dd, ^3J = 3.00 Hz, ^4J = 1.50 Hz), 1.77 (1H, d, ^2J = 8.85 Hz), 1.60 (1H, d, ^2J = 8.85 Hz), 1.36 (3H, t, ^3J = 7.10 Hz) ppm; ^{13}C NMR (75 MHz, $CDCl_3$): δ = 176.6, 165.9, 135.9, 134.9, 134.88, 130.5, 126.6, 61.4, 52.5, 46.1, 46.09, 14.5 ppm.

(3aR,4S*,7R*,7aS*)-3a,4,7,7a-Tetrahydro-2-phenyl-4,7-methano-1H-isoindole-1,3(2H)-dione* (**9e**)

From the general method, with 0.25 cm^3 of **3e** (2.68 mmol), 263 mg of maleic anhydride (2.68 mmol), and 0.45 cm^3 of cyclopentadiene (**8**, 5.36 mmol); the product was recrystallized from a cold mixture of CH_2Cl_2/*n*-hexane, leading to a yellow powder in 83.5% yield (536 mg, 2.24 mmol). M.p.: 136–138 °C (Ref. [45] 143 °C).

(3aR,4S*,7R*,7aS*)-2-(4-Fluorophenyl)-3a,4,7,7a-tetrahydro-4,7-methano-1H-isoindole-1,3(2H)-dione* (**9f**)

From the general method, with 0.22 cm^3 of **3f** (2.25 mmol), 220 mg of maleic anhydride (2.25 mmol), and 0.40 cm^3 of cyclopentadiene (**8**, 4.50 mmol); the product was recrystallized from a cold mixture of AcOEt/*n*-hexane, leading to a transparent crystals in 89.9% yield (520 mg, 2.02 mmol). M.p.: 172–174 °C (Ref. [46] 170–173 °C).

*General method for the preparation of the N-arylmaleamic acids **5a–5d***

The aniline **3a–3d** (2 g) and approximately 1.1 equivalents of maleic anhydride (**1**) were dissolved separately in 100-cm^3 round-bottom flasks fitted with rubber septa, with approximately 20 cm^3 of anhydrous THF each. The flask with the aniline, which also contained a magnetic stirrer, was introduced into an ice bath at 0 °C, and the solution of maleic anhydride was slowly added through a cannula. The mixture was stirred for 16 h at r.t., after which the product was filtered and washed twice with 20 cm^3 of *n*-hexane and characterized by spectroscopy. No further purification was carried out.

4-[[(2Z)-3-Carboxy-1-oxo-2-propen-1-yl]amino]benzoic acid (**5a**)
From the general method, with 2.0 g of **3a** (0.0146 mol) and 1.57 g of **1** (0.0163 mol); the reaction produced a yellow powder in 90.3% yield (3.10 g, 0.0132 mol). M.p.: 215–216 °C (Ref. [47]: 214–216 °C).

Ethyl 4-[[(2Z)-3-carboxy-1-oxo-2-propen-1-yl]amino]benzoate (**5b**)
From the general method, with 2.0 g of **3b** (0.0121 mol) and 1.30 g of **1** (0.0133 mol); the reaction produced a white powder in 89.0% yield (2.84 g, 0.0107 mol). M.p.: 177–179 °C (Ref. [48]: 194–196 °C).

3-[[(2Z)-3-Carboxy-1-oxo-2-propen-1-yl]amino]benzoic acid (**5c**)
From the general method, with 2.0 g of **3c** (0.0146 mol) and 1.57 g of **1** (0.0163 mol); the reaction produced a beige powder in 95.8% yield (3.05 g, 0.0116 mol). M.p.: 215–217 °C (Ref. [42]: 218–220 °C).

Ethyl 3-[[(2Z)-3-carboxy-1-oxo-2-propen-1-yl]amino]-benzoate (**5d**, $C_{13}H_{13}NO_5$)
From the general method, with 2.0 g of **3d** (0.0121 mol) and 1.30 g of **1** (0.0133 mol); the reaction produced a white powder in 77.7% yield (2.47 g, 0.0094 mol). M.p.: 155–158 °C; $R_f = 0.75$ (AcOEt/MeOH 1:1); UV–Vis (MeOH): λ_{max} (ε) = 217.3 ± 0.6 (37617.1) nm (mol^{-1} dm^3 cm^{-1}); IR (KBr): $\bar{\nu}$ = 3,312, 1,724, 1,683, 1,592, 1,580, 1,289, 1,112, 848, 761 cm^{-1}; ^{1}H NMR (300 MHz, DMSO-d_6): δ = 10.56 (1H, s), 8.28 (1H, s), 7.86 (1H, d, ^3J = 7.80 Hz), 7.66 (1H, d, ^3J = 7.80 Hz), 7.46 (1H, t), 6.47 (1H, d, ^3J = 12.00 Hz), 6.32 (1H, d, ^3J = 12.00 Hz), 4.30 (2H, q), 1.30 (3H, t) ppm; ^{13}C NMR (75 MHz, DMSO-d_6): δ = 167.7, 166.2, 164.2, 139.7, 132.2, 131.4, 131.0, 129.9, 125.0, 124.5, 120.5, 61.8, 14.5 ppm.

*General method for the preparation of Diels–Alder adducts **4a–4d** from arylmaleamic acids and isoprene*

The corresponding *N*-arylmaleamic acid **5a–5d** (250 mg) together with 2 equivalents of isoprene (**2**) and 9.0 cm^3 of toluene were deposited in a 20-cm^3 ACE pressure tube. The tube was closed, introduced into a sand bath at 160 °C, and kept under constant stirring for 96 h. After this time the product was precipitated with cold *n*-hexane, filtered, and washed twice with 20 cm^3 of *n*-hexane at r.t. The product was purified and characterized by spectroscopy.

*Diels–Alder adduct **4a***
From the general method, with 250 mg of **5a** (1.063 mmol) and 0.21 cm^3 of **2** (2.13 mmol); the product was recrystalized from a cold mixture of CH_2Cl_2/*n*-hexane, leading to a white powder in 76.8% yield (232.9 mg, 0.816 mmol).

*Diels–Alder adduct **4b***
From the general method, with 250 mg of **5b** (0.950 mmol) and 0.19 cm^3 of **2** (1.90 mmol); the product was recrystallized from a cold mixture of CH_2Cl_2/*n*-hexane, leading to a white powder in 82.7% yield (246.2 mg, 0.786 mmol).

*Diels–Alder adduct **4c***
From the general method, with 250 mg of **5c** (1.063 mmol) and 0.21 cm^3 of **2** (2.13 mmol); the product was recrystallized from a cold mixture of CH_2Cl_2/*n*-hexane, leading to a beige powder in 90.2% yield (273.5 mg, 0.959 mmol).

*Diels–Alder adduct **4d***
From the general method, with 250 mg of **5d** (0.950 mmol) and 0.19 cm^3 of **2** (1.90 mmol); the product was dissolved with CH_2Cl_2 and filtered through a layer of silica gel. The solvent was removed under vacuum in a rotary evaporator, leaving a translucent yellow liquid in 64.2% yield (231.2 mg, 0.738 mmol).

Theoretical methodology

The calculations described herein were carried out using the Gaussian 09 program package [27]. The optimizations were carried out using the TIGHT option; all DFT calculations were done using the INT(GRID = ULTRAFINE) option. The four conformers under study were drawn with Molden [49] and optimized first at the HF/STO-3G level of ab initio theory. The resulting geometries were used as starting points for subsequent optimizations at the HF/3-21G, HF/6-31+G(d,p), B3LYP/6-31+G(d,p), M06-2X/6-31+G(d,p), and M06-2X/6-31+G(d,p)/PCM levels of theory. For the PCM calculations the keyword SCRF (SOLVENT = CHLOROFORM) was used. At the highest levels employed we carried out vibrational analyses (25 °C, 1 bar) in order to obtain the corresponding free energy corrections to the electronic energies; no correction factors were applied to the vibrational frequencies. Only real frequencies were obtained for all optimized geometries. The dihedral angles relating to the coupling constants under study were measured with Molden on the geometries optimized at the highest levels of theory. From these angles an empirical set of coupling constants were obtained for each one of the conformers with the ALTONA computer program [33]. In addition, for each conformer we calculated the theoretical spin–spin coupling constants at the B3LYP/6-311+G(d,p)/PCM level of theory, according to the two-step methodology (Gaussian 09 keyword NMR = MIXED) described by Deng and co-workers [34]; only the coupling constants corresponding to the protons shown in Scheme 2 were calculated. For both sets of coupling constants the corresponding average values were calculated assuming a Boltzmann distribution of conformers from the estimated relative energies. Cartesian

coordinates of the conformers of **4a** along with absolute energies and lowest vibrational frequencies are given in the Supplementary Material.

Single-crystal X-ray crystallography

Recrystallization of adduct **9f** from CH_2Cl_2/*n*-hexane led to the formation of colorless crystals, one of which was mounted on a glass fiber. Crystallographic measurements were carried out at room temperature on an Oxford Diffraction Xcalibur S diffractometer using Mo Kα radiation (graphite monochromator, $\lambda = 0.71073$ Å), and a CCD detector. No absorption correction was applied. The structure was solved with SIR92 [50] and refined with SHELXL [51]. Anisotropic temperature factors were introduced for all non-hydrogen atoms. Hydrogen atoms were placed in idealized positions and their atomic coordinates refined. Unit weights were used in the refinement. The plot in Fig. 2 was made with ORTEP-3 for Windows (version 2.02) [52]. Data for adduct **9f** are summarized in Table 6. Supplementary crystallographic data have been deposited at the Cambridge Crystallographic Data Centre (CCDC 816697) [53].

Table 6 Crystallographic data of adduct **9f**

Empirical formula	$C_{15}H_{12}FNO_2$
Formula mass	313.34
Color	Colorless, prism
Crystal dimensions (mm)	0.21 × 0.23 × 0.30
Crystal system	Monoclinic
Space group	$P2_1/c$
Z	4
a (Å)	6.2846(1)
b (Å)	18.2110(3)
c (Å)	11.2899(3)
α (°)	90
β (°)	106.131(2)
γ (°)	90
Collection ranges	$-8 \leq h \leq 8$; $-23 \leq k \leq 23$; $-14 \leq l \leq 14$
Temperature (K)	292(2)
Volume (Å^3)	1,241.24(4)
D_{calcd} (mg m^{-3})	1.377
Radiation	Mo Kα ($\lambda = 0.71073$ Å)
Absorption coeff. (μ) (mm^{-1})	0.102
Absorption correction	None
$F(000)$	536
T range for data collection (°)	2.92–27.75
Observed reflections	13,528
Independent reflections	2,906 ($R_{int} = 0.0575$)
Data/restraints/parameters	2,906/0/173
Goodness-of-fit on F^2	1.097
Final R indices [$I > 2\sigma(I)$]	$R_1 = 0.0855$, $wR_2 = 0.1901$
R indices (all data)	$R_1 = 0.0973$, $wR_2 = 0.1994$
Absolute structure parameter	N/a
Extinction coefficient	4.7(2)
Largest diff. peak and hole (e Å^{-3})	0.425 and −0.463

Acknowledgements We thank the Secretaría de Investigación y Posgrado of the Instituto Politécnico Nacional for financial support (Grants: DQZ, 20110101; HAJV, 20100506; JTF, 20100220). DQZ and HAJV are fellows of the COFAA and EDI programs of the IPN. JAGS thanks the Consejo Nacional de Ciencia y Tecnología for the award of a scholarship. We thank Francisco Ayala M.Sc. for the HRMS measurements and Profs. G. Zepeda and J. Tamariz for helpful comments.

References

1. González-López M, Shaw JT (2009) Chem Rev 109:164
2. Khadem S, Udachin KA, Enright GD, Prakesch M, Arya P (2009) Tetrahedron Lett 50:6661
3. Sato S, Isobe H, Tanaka T, Ushijima T, Nakamura E (2005) Tetrahedron 61:11449
4. Wright DL, Robotham CV, Aboud K (2002) Tetrahedron Lett 43:943
5. Ramachary DB, Barbas CF (2004) Chem Eur J 10:5323
6. Smith CD, Gavrilyuk JI, Lough AJ, Batey RA (2010) J Org Chem 75:702
7. Smith BM, March J (2001) March's advanced organic chemistry, 5th edn. Wiley, New York
8. Mukherjee S, Corey EJ (2010) Org Lett 12:632
9. Soh JY-T, Tan C-H (2009) J Am Chem Soc 131:6904
10. Kiriazis A, Leikoski T, Mutikainen I, Yli-Kauhaluoma J (2004) J Comb Chem 6:283
11. Sanyal A, Snyder JK (2000) Org Lett 2:2527
12. Goh YW, Pool BR, White JM (2008) J Org Chem 73:151
13. Schwarzer A, Bombicz P, Weber E (2010) J Fluorine Chem 131:345
14. Hill KW, Taunton-Rigby J, Carter JD, Kropp E, Vagle K, Pieken W, McGee DPC, Husar GM, Leuck M, Anziano DJ, Sebesta DP (2001) J Org Chem 66:5352
15. Lei X, Porco JA (2004) Org Lett 6:795
16. Lambert JB, Marko DE (1985) J Am Chem Soc 107:7978
17. Vereshchagin AN (1983) Russ Chem Rev 52:1081
18. Anastas'eva AP, Vereshchagin AN, Arbuzov BA (1970) Izv Akad Nauk SSSR, Ser Khim 1709
19. Bennett DJ, Craig AC, Mundy BP, Dirks GW, Lipkowitz KB (1976) J Org Chem 41:469
20. Larter RM, Craig RER, Craig AC, Mundy BP (1977) J Org Chem 42:1259
21. Odinokov VN, Galeeva RI, Tolstikov GA, Spirikhin LV, Zaev EE (1977) Zh Org Khim 13:1195
22. Timosheva AP, Vul'fson SG, Sorochinskaya EI, Vereshchagin AN, Arbuzov BA (1975) Izv Akad Nauk SSSR, Ser Khim 865
23. Vereshchagin AN, Anastas'eva AP, Arbuzov BA (1970) Izv Akad Nauk SSSR, Ser Khim 995
24. Chopra D, Mohan TP, Rao KS, Guru Row TN (2004) Acta Crystallogr E60:o2406
25. Kishikawa K, Naruse M, Kohmoto S, Yamamoto M, Yamaguchi K (2001) J Chem Soc Perkin Trans 1 462
26. Smith GD, Otzenberger RD, Mundy BP, Caughlan CN (1974) J Org Chem 39:321

27. Frisch MJ, Trucks GW, Schlegel HB, Scuseria GE, Robb MA, Cheeseman JR, Scalmani G, Barone V, Mennucci B, Petersson GA, Nakatsuji H, Caricato M, Li X, Hratchian HP, Izmaylov AF, Bloino J, Zheng G, Sonnenberg JL, Hada M, Ehara M, Toyota K, Fukuda R, Hasegawa J, Ishida M, Nakajima T, Honda Y, Kitao O, Nakai H, Vreven T, Montgomery JA Jr, Peralta JE, Ogliaro F, Bearpark M, Heyd JJ, Brothers E, Kudin KN, Staroverov VN, Keith T, Kobayashi R, Normand J, Raghavachari K, Rendell A, Burant JC, Iyengar SS, Tomasi J, Cossi M, Rega N, Millam JM, Klene M, Knox JE, Cross JB, Bakken V, Adamo C, Jaramillo J, Gomperts R, Stratmann RE, Yazyev O, Austin AJ, Cammi R, Pomelli C, Ochterski JW, Martin RL, Morokuma K, Zakrzewski VG, Voth GA, Salvador P, Dannenberg JJ, Dapprich S, Daniels AD, Farkas O, Foresman JB, Ortiz JV, Cioslowski J, Fox DJ (2010) Gaussian 09 Revision B.01
28. Zhao Y, Truhlar D (2008) Theor Chem Acc 120:215
29. Zhao Y, Truhlar DG (2011) J Chem Theory Comput 7:669. doi: 10.1021/ct1006604
30. Tomasi J, Mennucci B, Cammi R (2005) Chem Rev 105:2999
31. Scalmani G, Frisch MJ (2010) J Chem Phys 132:114110
32. Haasnoot CAG, de Leeuw FAAM, Altona C (1980) Tetrahedron 36:2783
33. Cerda-García-Rojas C, Zepeda LG, Joseph-Nathan P (1990) Tetrahedron Comput Method 3:113
34. Deng W, Cheeseman JR, Frisch MJ (2006) J Chem Theor Comput 2:1028
35. Herrera R, Jiménez-Vázquez HA, Tamariz J (2005) ARKIVOC 233
36. Augustin M (1985) Z Chem 25:18
37. Correa-Basurto J, Vázquez Alcántara I, Espinoza-Fonseca LM, Trujillo-Ferrara JG (2005) Eur J Med Chem 40:732
38. Fruk L, Graham D (2003) Heterocycles 60:2305
39. Liu K, Lu H, Hou L, Qi Z, Teixeira C, Barbault F, Fan B-T, Liu S, Jiang S, Xie L (2008) J Med Chem 51:7843
40. Paterson MJ, Eggleston IM (2008) Synth Commun 38:303
41. Trujillo-Ferrara J, Correa-Basurto J, Espinosa J, García J, Martínez F, Miranda R (2005) Synth Commun 35:2017
42. Trujillo-Ferrara J, Montoya Cano L, Espinoza-Fonseca M (2003) Chem Lett 13:1825
43. Trujillo-Ferrara J, Vázquez I, Espinosa J, Santillan R, Farfán N, Höpfl H (2003) Eur J Pharm Sci 18:313
44. Fringuelli F, Girotti R, Pizzo F, Vaccaro L (2006) Org Lett 8:2487
45. Billett NG, Phillis AT, Main L, Nicholson BK, Denny WA, Hay MP (2006) ARKIVOC (iii):184
46. Vargas J, Santiago AA, Gaviño R, Cerda AM, Tlenkopatchev MA (2007) Express Polym Lett 1:274
47. Koechel DA, Tarloff JB, Rankin GO (1983) J Med Chem 26:85
48. Kolyamshin OA, Danilov VA, Kol'tsov NI (2007) Russ J Org Chem 43:393
49. Schaftenaar G, Noordik JH (2000) J Comput-Aided Mol Des 14:123
50. Altomare A, Cascarano G, Giacovazzo C, Guagliardi A (1993) SIR92. J Appl Crystallogr 26:343
51. Sheldrick GM (2008) SHELXL-97 release 97-2. Acta Crystallogr A 64:112
52. Farrugia LJ (1997) ORTEP-3 for Windows. J Appl Crystallogr 30:565
53. These data can be obtained free of charge from the CCDC through the web page: http://www.ccdc.cam.ac.uk/data_request/cif